ELSEVIER

International Journal of Heat and Fluid Flow 23 (2002) 373–379

International Journal of HEAT AND FLUID FLOW

www.elsevier.com/locate/ijhff

Numerical model to study natural convection in a rectangular enclosure filled with two immiscible fluids ☆

Nikolay P. Moshkin *,1

School of Mathematics, Institute of Science, Suranaree University of Technology, Nakhon Ratchasima 30000, Thailand

Abstract

A finite-difference approximation of the Navier–Stokes equations under the Boussinesq-fluid assumption is used to simulate the flow and heat transfer in a two-layer system of an immiscible incompressible fluid. The numerical model is validated with a benchmark solution which is buoyancy-driven flow in a square cavity with differently heated vertical sides. The results of the two-dimensional numerical simulation are compared with the experimental data of the hydrodynamics and heat exchange within a horizontal two-layer medium consisting of two immiscible liquids of different densities and viscosities. Comparisons are made for the profiles of the temperature and for the profiles of the horizontal and vertical components of the velocity vector as well. Qualitative agreement between numerical and experimental results is observed.

Keywords: Natural convection; Two-layer; Two-dimensional numerical simulation

1. Introduction

The study of thermal convection in two-layer systems of immiscible liquids was inspired by numerous applications of this problem, such as the development of liquid encapsulated crystal growth techniques, the problem of mantle convection, as well as many others.

An excellent survey of work on the convection in a two-layer system of immiscible liquids up to 1994 has been provided by Prakash and Koster (1996, 1997). Parametric studies have been performed by many researchers to understand the physics and mechanisms of natural convection in a two-layer system of immiscible fluids. They observe, that two distinct coupling models between the layers exist. These coupling models are mechanical (or viscous) coupling and thermal coupling. The viscosity ratio, and the ratio of driving forces between the two liquids have the largest influence on the coupling mechanism.

Mantle convection is now a generally accepted principle of geodynamics. Thermal convection in the mantle drives plate tectonics. Knowledge of mantle dynamics and the constitution of the deeper mantle is important in trying to understand a number of aspects of plate tectonics. There are several models of mantle convection. One of these models assumes that convection takes place in two discrete layers, the upper and lower mantle, and that there is no significant mass transfer across the boundary between them. For instance, this problem was studied by Richer (1979), Richer and McKenzie (1981), Dobretsov and Kyrdyashkin (1993), Csereper and Rabinovicz (1985/86), and Csereper et al. (1988).

The results of numerical simulation depend on many general assumptions and realizations of the boundary conditions. Some inconsistencies always exist between experiments and two-dimensional numerical simulations. Therefore, there is a need for numerical methods that establish a link between numerical simulation and laboratory experiment. It is the purpose of the present research to study a finite-difference method which generates numerical approximation to the experimental data. Here, a numerical model for the study of thermal convection in two-layers is presented, and the results of the two-dimensional numerical simulations are

☆ This paper is a revised and expanded version of a paper presented at CHT'01, the Second International Symposium on Advances in Computational Heat Transfer (Palm Cove, Qld., Australia, 20–25 May 2001), the proceedings of which were published by Begell House, Inc.

* Tel.: +66-44-224-382; fax: +66-44-224-185.

E-mail address: moshkin@math.sut.ac.th (N.P. Moshkin).

[1] The author is on leave from Institute of Computational Technologies, Russian Academy of Science, Novosibirsk, Russia.

0142-727X/02/$ - see front matter
PII: S0142-727X(02)00185-6

compared with the experimental data of Dobretsov and Kyrdyashkin (1993).

2. Equations of mathematical model

The problem of convection has been thoroughly investigated in a number of research articles. Let us list here the basic equations and the boundary conditions. The equations of the Boussinesq approximation, in terms of velocity and pressure, are

$$\frac{\partial u_i}{\partial t}+u_k\frac{\partial u_i}{\partial x_k}=-c'\frac{\partial p}{\partial x_i}+\frac{Pr}{c}\frac{\partial \sigma_{ik}}{\partial x_k}+\frac{Ra\,Pr}{c^2}Tg_i, \tag{1}$$

$$\sigma_{ik}=\mu(x_1,x_2,T,p)\left(\frac{\partial u_i}{\partial x_k}+\frac{\partial u_k}{\partial x_i}\right),$$

$$\frac{\partial T}{\partial t}+u_k\frac{\partial T}{\partial x_k}=\frac{1}{c}\frac{\partial^2 T}{\partial x_k\,\partial x_k}, \tag{2}$$

$$\frac{\partial u_k}{\partial x_k}=0,\quad i,k=1,2;\quad g=(0,g_2), \tag{3}$$

where $x_1=x$ and $x_2=z$ are the Cartesian coordinates, $u_1=u$ and $u_2=v$ are the horizontal and vertical components of the velocity vector, respectively, p is the pressure, t is the time, g_2 is the acceleration of gravity, T is the fluid temperature, μ is the coefficient of dynamic viscosity, c and c' are the scaling factors. The governing equations are scaled using the thermal properties of layers, the container's height H, and the temperature difference. The following time, velocity, pressure, temperature and viscosity scales are used

$$t'=c\frac{\alpha}{H^2}t,\quad u_i'=c^{-1}\frac{H}{\alpha}u_i;\quad i=1,2;$$

$$p'=\frac{H^2}{\rho\alpha^2c^2c'}p,\quad T'=\frac{T-T_0}{T_1-T_0},\quad \mu'=\frac{\mu}{\mu_2}.$$

Here H is the length scale, α is the coefficient of the thermal diffusivity, ρ is the density of the fluids, T_0 and T_1 are the temperatures of the upper and lower boundaries, respectively, and c is a non-dimensional scalar which is chosen as $c=1$ or $c=Pr$. The non-dimensional parameters appearing in the above mentioned problem are

$$x_l=\frac{L}{H},\quad Ra=\frac{g\beta T_1H^3}{\alpha\nu},\quad Pr=\frac{\nu}{\alpha},$$

the aspect ratio, the Rayleigh number and the Prandtl number, respectively (β is the coefficient of thermal expansion).

A two-dimensional rectangular cavity with aspect ratio H/L is considered. The origin of the coordinate system is placed at the lower left corner of the container. The heights of the two layers are not necessarily equal. Each layer consists of a fluid of constant viscosity. The way in which the two layers may differ is in their viscosity. The kinematic viscosities of the upper and lower layers are ν_1 and ν_2, respectively. Mechanically, the boundaries of the box are no-slip boundaries. The upper and lower horizontal boundaries are isothermal surfaces. The vertical walls are insulated. The interface between the layers is fixed at the depth $z=z_d=d$, $0<d<1$. There is no mass flux across the interface boundary. The tangential velocity components and tangential stresses are continuous at $z=z_d$.

The governing Eqs. (1)–(3) are supplemented by the following boundary conditions. The upper and lower boundaries are isothermal surfaces with no-slip boundary conditions

$$T=0 \text{ at } z=0,\quad 0\leqslant x\leqslant x_l,$$

$$T=1 \text{ at } z=1,\quad 0\leqslant x\leqslant x_l,$$

$$v=0,\ u=0 \text{ at } z=0,\ z=1 \text{ and } 0\leqslant x\leqslant x_l.$$

The vertical sides of the box are insulated

$$\frac{\partial T}{\partial x}=0 \text{ at } x=0,\quad x=x_l \text{ and } 0\leqslant z\leqslant 1,$$

and mechanically they are no-slip boundaries

$$u=0,\quad v=0 \text{ at } x=0,\quad x=x_l \text{ and } 0\leqslant z\leqslant 1.$$

The boundary conditions at the interface boundary prescribe the continuity of the horizontal velocity and the continuity of the tangential stresses and exclude fluid motion across the interface

$$v=0,\quad [u]=u(x,d-0)-u(x,d+0)=0,$$

$$\left[\nu\frac{\partial u}{\partial z}\right]=0 \text{ at } z=d,\ 0\leqslant x\leqslant x_l.$$

3. Numerical model

When using the equations of fluid dynamics in primitive (velocity–pressure) variables the main idea in the construction of a numerical method is that the pressure in a subsequent time level may be determined by the vanishing of the divergence of the velocity vector (MAC method Harlow and Welch (1965)). The same idea was also realized in the splitting method of Belotserkovskii et al. (1975) in which the computation process is divided into three stages. An implicit method of the same class with pressure correction was studied by Tolstykh (1991).

The algorithm for the numerical solution of Eqs. (1)–(3) with boundary conditions presented above is based on the method of splitting in the physical process (Belotserkovskii et al., 1975). The approximation is carried out on a staggered grid ω_h, i.e. the pressure and temperature are specified at the centers of the cells and the velocity components are specified at the centers of the corresponding cell's surfaces.

The boundary, which separates the two fluids, passes through the grid line where the vertical component of the velocity vector is defined. Let j_d be the number of the horizontal grid line corresponding to this boundary. It follows from the boundary conditions that $v_{i,j_d} = 0$ on this boundary. The two tangent components of the velocity vector on the different sides of the interface boundary, $z = d$, are $u^+ = u(x, d+0)$ and $u^- = u(x, d-0)$. The approximation of the boundary conditions $[v(\partial u/\partial z)] = 0$ and $[u] = 0$ may be expressed in the following form

$$\begin{cases} v_1\left[\sum\limits_{m=1}^{N^+} C_m^+ u_{i+1/2,j_d+m} + C^+u^+\right] = v_2\left[\sum\limits_{m=1}^{N^-} C_m^- u_{i+1/2,j_d-m} + C^-u^-\right], \\ u^+ = u^-, \end{cases} \tag{4}$$

where

$$\left(\frac{\partial u}{\partial z}\right)_{z=d-0} = \sum_{m=1}^{N^-} C_m^- u_{i+1/2,j_d-m} + C^-u^- + O(h^\beta),$$

$$\left(\frac{\partial u}{\partial z}\right)_{z=d+0} = \sum_{m=1}^{N^+} C_m^+ u_{i+1/2,j_d+m} + C^+u^+ + O(h^\alpha).$$

Here N^+, N^- are the number of grid points used to approximate the partial derivatives by one-sided differences. These two Eq. (4) can be solved with respect to $u^+ = u^- = u_\gamma$

$$u_\gamma = \frac{v_1\sum\limits_{m=1}^{N^+} C_m^+ u_{i+1/2,j_d+m} - v_2\sum\limits_{m=1}^{N^-} C_m^- u_{i+1/2,j_d-m}}{v_1C^+ - v_2C^-}.$$

This is a reduced boundary condition on the boundary which separates two fluids.

In order to describe the numerical methods it is convenient to present the momentum and continuity equations in vector form

$$\frac{\partial \mathbf{u}}{\partial t} + L\mathbf{u} = -\frac{1}{\rho}\nabla p, \tag{5}$$

$$\mathrm{div}\mathbf{u} = 0. \tag{6}$$

Here, the operator L contains convective and diffusive terms. Introducing the difference analogues L_h, div_h, and ∇_h of the operators L, div, and ∇ on the grid ω_h, the following approximations of (5), (6) are used

$$\begin{aligned} &\mathbf{u}^* - \mathbf{u}^n + \tau L_h\mathbf{u}^* = -\tau\,\tfrac{1}{\rho}\mathrm{grad}_h\, p^n, \\ &\mathbf{u}^{n+1} = \mathbf{u}^* - \tau\tfrac{1}{\rho}\mathrm{grad}_h\,\delta p, \quad \mathrm{div}_h\,\mathbf{u}^{n+1} = 0, \\ &\tfrac{1}{\rho}\mathrm{div}_h\mathrm{grad}_h\,\delta p = \tfrac{1}{\tau}\mathrm{div}_h\,\mathbf{u}^*, \quad \delta p = p^{n+1} - p^n. \end{aligned} \tag{7}$$

Here, δp is the correction of the pressure, $\mathbf{u}^*$ is the vector of the preliminary values of velocity which has to be corrected. Thus, in order to find the velocity and pressure fields for $t = t_{n+1}$, one needs to solve the first equation of system (7) with respect to $\mathbf{u}^*$ and then to find δp from the last equation of system (7). The values of the velocities $\mathbf{u}^{n+1}$ are determined from the second equation of system (7). It should be emphasized here that the values of $\mathbf{u}^*$ are determined implicitly and have a physical rather than an artificial meaning.

The order of the spatial approximation of scheme (7) depends on the choice of the operator L_h. The Poisson equation arises for the pressure correction δp. The boundary conditions for the pressure correction can be reduced to the finite-difference analogue of the homogeneous conditions of Neuman type. The Neuman problem obtained in this way has a solution only if the total fluid flux across all outer boundaries is equal to zero. The solution of the boundary value problem for the Poisson equation is obtained by means of the iterative scheme of stabilizing corrections (Yanenko, 1971). The temperature field T at the grid points is defined either by the implicit finite difference scheme of stabilizing correction or by the predictor corrector scheme (Yanenko, 1971).

The method of stabilizing corrections is a very general and effective method for the solution of the heat transfer equations. In the case of Eq. (2) this method has the following form

$$\begin{aligned} \frac{\widetilde{T}_{i,j} - T^n_{i,j}}{\Delta t} &= -\frac{(uT)^n_{i+1/2,j} - (uT)^n_{i-1/2,j}}{h_x} \\ &\quad - \frac{(vT)^n_{i,j+1/2} - (vT)^n_{i,j-1/2}}{h_z} \\ &\quad + \frac{1}{c}\left[\frac{T^n_{i+1,j} - 2T^n_{i,j} + T^n_{i-1,j}}{h_x^2}\right. \\ &\quad \left. + \frac{\widetilde{T}_{i,j+1} - 2\widetilde{T}_{i,j} + \widetilde{T}_{i,j-1}}{h_z^2}\right], \\ \frac{T^{n+1}_{i,j} - \widetilde{T}_{i,j}}{\Delta t} &= \frac{1}{c}\left[\frac{T^{n+1}_{i+1,j} - 2T^{n+1}_{i,j} + T^{n+1}_{i-1,j}}{h_x^2}\right. \\ &\quad \left. - \frac{T^n_{i+1,j} - 2T^n_{i,j} + T^n_{i-1,j}}{h_z^2}\right]. \end{aligned}$$

The first fractional step produces absolute consistency with Eq. (2) and the next fractional step serves to improve the stability.

The finite-difference scheme for Eq. (2) which is based on the predictor–corrector principle has the following form

$$\begin{aligned} \frac{T^{n+1/3}_{i,j} - T^n_{i,j}}{0.5\Delta t} &= -\left(\frac{\partial vT}{\partial z}\right)^h_{i,j} \\ &\quad + \frac{1}{c}\frac{T^{n+1/3}_{i,j+1} - 2T^{n+1/3}_{i,j} + T^{n+1/3}_{i,j-1}}{h_z^2} \\ &= \Lambda_{zz}T^{n+1/3}_{i,j}, \end{aligned} \tag{8}$$

$$\frac{T_{i,j}^{n+2/3}-T_{i,j}^{n+1/3}}{0.5\Delta t}=-\left(\frac{\partial uT}{\partial x}\right)_{i,j}^{h}+\frac{1}{c}\frac{T_{i+1,j}^{n+2/3}-2T_{i,j}^{n+2/3}+T_{i-1,j}^{n+2/3}}{h_x^2}=\Lambda_{xx}T_{i,j}^{n+2/3}, \tag{9}$$

$$\frac{T_{i,j}^{n+1}-T_{i,j}^{n}}{\Delta t}=(\Lambda_{zz}+\Lambda_{xx})T_{i,j}^{n+2/3}, \tag{10}$$

where the upper index h in Eqs. (8) and (9) denotes a finite difference approximation at the grid point i,j of the corresponding derivative. Eqs. (8) and (9) represent the predictor, based on an implicit splitting scheme, and Eq. (10) is the corrector.

4. Solution of the bench mark problem

Computations was first performed for the widely used benchmark problem of a buoyancy-driven flow in a square cavity (de Vahl Davis, 1983; de Vahl Davis and Jones, 1983). The problem considered is that of the two-dimensional flow of a Boussinesq fluid of Prandtl number 0.71 in an upright square cavity of side L. Both velocity components are zero on the boundaries. The horizontal walls are insulated and the vertical sides are at different temperatures. The solution of this problem (velocities, temperature and rates of heat transfer) has been obtained at Rayleigh numbers of $Ra=10^3$, 10^4, 10^5, 10^6. The benchmark values and results of the recent numerical experiments appear in Table 1.

In Table 1, $Nu_{\max}$ is the maximum value of the local Nusselt number on the boundary at $x=0$, $\overline{Nu}=\int_0^1(\partial T/\partial x)\mathrm{d}z\,|_{x=0}$ is the average Nusselt number, and $u_{\max}$ is the maximum horizontal velocity on the vertical mid-plane of the cavity. The analysis of the data collected in Table 1 indicates an acceptable level of agreement between the benchmark and our computational results.

5. Comparison with laboratory experiment

In the experimental research of Dobretsov and Kyrdyashkin (1993) a two-layer model of mantle convection was derived from experimental work on hydrodynamics and heat exchange within a horizontal two-layer medium consisting of two immiscible liquids of different densities and viscosities, the upper one cooled and the lower one heated. The viscosity of the thinner upper layer is less than that of the lower layer. Two immiscible liquids, glycerin and hexadecan, were used in the experiments. Hexadecan has the following properties at $T=30$ °C: the density, ρ, is 766.5 kg/m^3; the thermoconductivity, k, is 0.147 W m^{-1} °C^{-1}; the dynamic viscosity, μ, is 2.754×10^{-3} N s m^{-2}; the kinematic viscosity, v, is 0.359×10^{-5} m^2 s^{-1}; the thermal diffusivity, α, is 1.154×10^{-7} m^2 s^{-1}; the coefficient of thermal expansion, β, is 0.529×10^{-3} °C^{-1}; the Prandtl number, $Pr=v/\alpha$ is 31.13. Glycerin has the following physical properties at $T=40$ °C: $\rho=1259$ kg/m^3; $k=0.283$ W m^{-1} °C^{-1}; $\mu=330\times10^{-3}$ N s m^{-2}; $v=2.64\times10^{-4}$ m^2 s^{-1}; $\alpha=9.18\times10^{-8}$ m^2 s^{-1}; $\beta=4.4\times10^{-4}$ °C^{-1}; $Pr=2.88\times10^3$.

Experimental investigations were carried out when the layers have a thickness of $l_1/l_2\ll1$ and $v_1/v_2=73.5$. Fig. 1 shows the schematic representation of the stream lines in the two-layer system of liquids and also the cross-sections $A-A$ and $B-B$, where the velocity profiles are given in Figs. 3 and 4.

The main calculations were carried out on a grid of 52×200 nodes in the z and x directions, respectively. The aspect ratio of the domain $x_l=L/H$ corresponds to the size of the experimental box 100/26. The non-dimensional parameters are taken according to the conditions of the experiment and the physical properties of glycerin and hexadecan $Ra=38461.5$, $Pr=31.13$, $v_2/v_1=73.5$. Fig. 2 shows the quasi-steady solution in terms of the stream lines and isotherms. Note that the flow structure in the numerical simulations of the two-layer system is similar to the flow pattern in the laboratory experiment. Correlation between descending flows in the upper and lower layers, as well as between ascending flows, occurred in both the numerical simulations and in the experimental data.

Fig. 3 shows the profile of the horizontal component of the velocity in the liquid layers of glycerin ($l_2=19$ mm) and hexedecan ($l_1=7$ mm). The circles represent the experimental results and the solid line

Table 1
Comparison of the our numerical results with benchmark solution

Ra	10^3	10^4	10^5	10^6	
$Nu_{\max}$	1.505	3.528	7.717	17.925	Benchmark
$Nu_{\max}$	1.515	3.620	8.920	19.200	21×21
$Nu_{\max}$	1.510	3.581	7.530	17.237	41×41
$\overline{Nu}$	1.118	2.243	4.519	8.800	Benchmark
$\overline{Nu}$	1.111	2.222	5.150	10.900	21×21
$\overline{Nu}$	1.113	2.198	4.430	9.045	41×41
$u_{\max}$	3.649	16.178	34.73	64.63	Benchmark
$u_{\max}$	3.494	17.070	42.59	59.13	21×21
$u_{\max}$	3.650	16.875	37.75	61.18	41×41

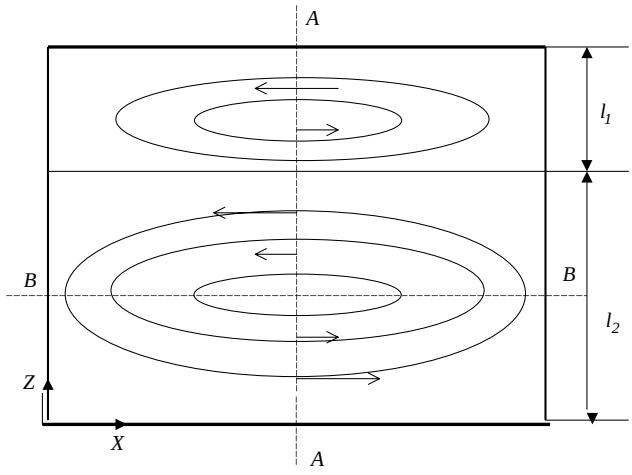

Fig. 1. Scheme of experimental lines of flow for one convective cell. Location of sections $A-A$ and $B-B$ where profiles of velocity components are displayed in Figs. 3 and 4.

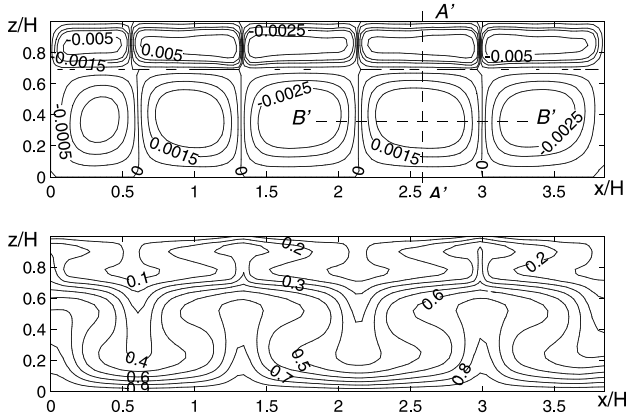

Fig. 2. Stream lines and isotherms. Results of the our numerical simulations. Location of sections $A'-A'$ and $B'-B'$ where profiles of velocity components are displayed in Figs. 3 and 5.

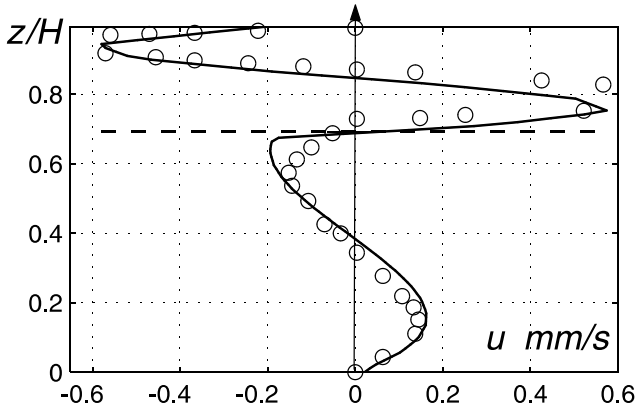

Fig. 3. Profile of the horizontal component of velocity at the sections $A-A$ and $A'-A'$, ($x = 2.5535$). (○) Experimental data, (—) our numerical simulation.

corresponds to the results of our numerical simulation. The experimental data correspond to the section $A-A$ which passes through the middle of the convection cells. This section is shown in Fig. 1. The computational results are represented at section $A'-A'$ which is given by the equation $x/H = 2.5535$. This section $A'-A'$ is shown in Fig. 2. Near the liquid interface boundary a counter current appears. As pointed out by Dobretsov and Kyrdyashkin (1993) the reason for the counter current is thermal coupling.

Fig. 4 shows the experimental profile of the vertical component of velocity for the section $B-B$, which corresponds to $z = z_d/2$. This section is shown on Fig. 1. Fig. 5 shows numerical profile of the vertical component of velocity for the section $B'-B'$, which is shown on Fig. 2.

Fig. 6 shows the experimentally measured temperature profiles at various vertical cross-sections parallel to the roll axis as well as the temperature profiles obtained by numerical simulation. The profile marked by a dashed line corresponds to the section $x = 2.1214$ in the region of descending flow. The profile marked by the dash-dotted line corresponds to the section $x = 2.9857$ located in the region of ascending flow. The solid line corresponds to the section $x = 2.5535$ in the region

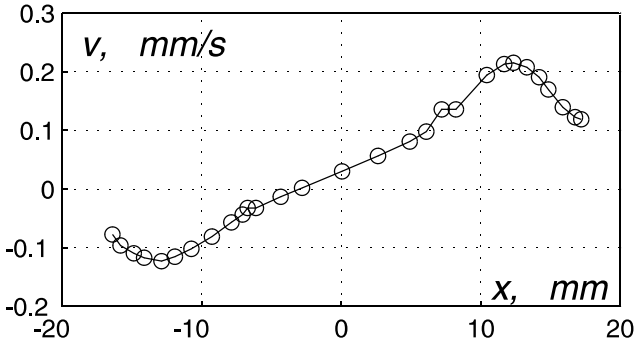

Fig. 4. Profile of the vertical component of velocity at the section $B-B$, $z = z_d/2$. Experimental results

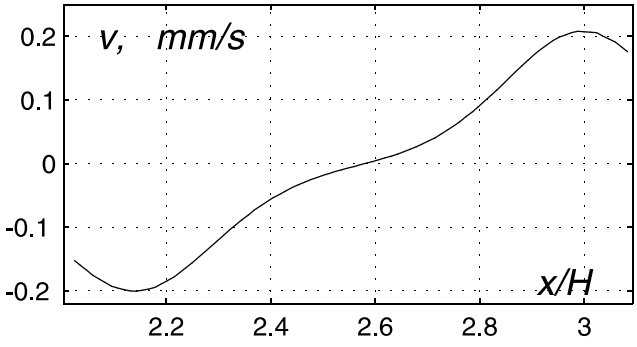

Fig. 5. Profile of the vertical component of velocity at the section $B'-B'$ (see Fig. 2). Results of numerical simulation.

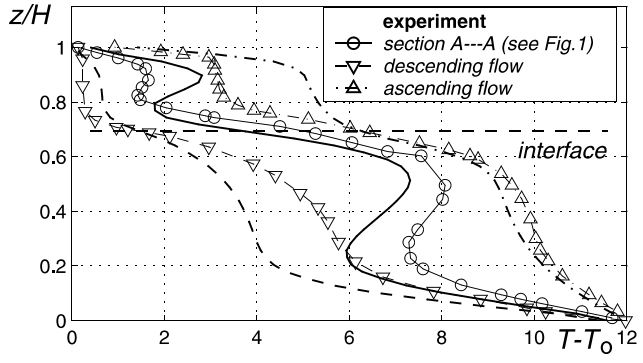

Fig. 6. Temperature profiles at several vertical cross-sections from descending flow to ascending flow. Results of the numerical simulations and experimental study of Dobretsov and Kyrdyashkin (1993).

closer to the section $A'-A'$ (see Fig. 2). The lines marked by upward triangles, by circles, and by downward triangles represent the experimental data of Dobretsov and Kyrdyashkin (1993).

As Fig. 3 shows, the numerical values of the maximum horizontal velocities are given by $u^{(1)}_{\max} = 0.6$ mm/s and $u^{(2)}_{\max} = 0.19$ mm/s for the thin layer of hexadecan and for the lower layer of glycerin, respectively. The experimental value $\widetilde{u}^{(1)}_{\max} = 0.8$ mm/s is greater and $\widetilde{u}^{(2)}_{\max} = 0.15$ mm/s is smaller then the corresponding values in the numerical simulation. At the same time, the maximum horizontal velocity of free convection in the single cell can be found from the relationship (see Dobretsov and Kyrdyashkin, 1993)

$$Pe_m = \frac{u_{\max} L}{\alpha} = 0.24(Ra\,Ra_c)^{1/2} \tag{11}$$

where $Pe_m = Re_m Pr$ is the Peclet number, Ra_c is the critical Rayleigh number, $Re_m = u_{\max} l/v$ is the Reynolds number, and $Pr = v/\alpha$ is the Prandtl number. This dependence is determined experimentally (Kutateladze et al., 1974; Berdnikov and Kyrdyashkin, 1990) within the range $Ra_c < Ra < 6 \times 10^4$, and theoretically by the method of finite amplitudes for the environment of the stability loss point $Ra = Ra_c$ (Chandrasekhar, 1961). The general temperature gradient in a two layer system is $\Delta T = 12$ °C. The average temperature of the liquid interface is 3.5 °C. Hence $\Delta T^{(1)} = 3.5$ °C, $\Delta T^{(2)} = 8.5$ °C, and according to the physical properties of the fluids we have $Ra^{(1)} = 1.5 \times 10^4$ and $Ra^{(2)} = 1.04 \times 10^4$ for the upper and the lower layer, respectively. The maximum velocities $\widehat{u}^{(1)}_{\max}$ and $\widehat{u}^{(2)}_{\max}$ from (11) are $\widehat{u}^{(1)}_{\max} = 0.46$ mm/s and $\widehat{u}^{(2)}_{\max} = 0.11$ mm/s. The values of the maximum velocities of the numerical model differ from the experimental ones by 25% for the upper and 21% for the lower layer. At the same time, the differences between $u^{(1)}_{\max}$ and $u^{(2)}_{\max}$ in the numerical model and those found from (11), $\widehat{u}^{(1)}_{\max}$ and $\widehat{u}^{(2)}_{\max}$ are 23% and 42%, respectively.

6. Conclusion

The problem of natural convection in a rectangular container filled with two immiscible fluids is investigated numerically by a finite-difference method. The numerical results for the velocity and temperature profiles are compared with experimental data. For the parameters used in the numerical and physical experiments a strict correlation between downward and upward flows is observed for the upper and lower layers. This correlation is due to the physical and geometrical conditions of convective flow where the thickness of the upper layer with less viscous fluid is significantly less than that of the lower layer.

The results of the numerical simulation reported here indicate only qualitative agreement with the experimental data. There are many reasons for the difference in the data obtained by the numerical and experimental simulations. The main reasons are probably due to the two dimensional model used as well as the boundary conditions on the interface boundary. However, it is hoped that the numerical model developed here can be considered a reasonable tool to simulate natural convective flows in a many-layered system of fluids.

Acknowledgements

The author wishes to thank Prof. N.L. Dobretsov and Prof. A.G. Kyrdyashkin for their attention and for useful discussions while working on this problem. These discussions stimulated interest in the problem of convective flows in two-layers fluids. Part of this work was supported by the Suranaree University of Technology, Nakhon Ratchasima, Thailand.

References

Belotserkovskii, O.M., Gushin, V.A., Shennikov, V.V., 1975. Splitting method applied to the problem of viscous incompressible liquid dynamics. ZhVMiMF 15, 197–207.

Berdnikov, V.S., Kyrdyashkin, A.G., 1990. Structure of free-convection flows in a horizontal layer of liquid under various boundary conditions. Fluid Mech. Sov. Res. 9, 1–36.

Dobretsov, N.L., Kyrdyashkin, A.G., 1993. Experimental modelling of two-layer mantel convection. Ofoliti 18 (1), 61–81.

Chandrasekhar, S., 1961. Hydrodynamic and hydromagnetics stability. Clarendon, Oxford.

Csereper, L., Rabinovicz, M., 1985/86. Gravity and convection in two-layer mantle. Earth Planet. Sci. Lett. 76, 193–207.

Csereper, L., Rabinovicz, M., Rosemberg-Borot, C., 1988. Three-dimensional infinite Prandtl number convection in one and two-layers with applications for the Earth's gravity field. J. Geophys. Res. 93, 12009–12025.

Harlow, T., Welch, J.E., 1965. Numerical calculation of time dependent viscous incompressible flow of fluid with free surface. Phys. Fluids 8, 2182–2189.

Kutateladze, S.S., Kirdyashkin, A.G., Berdnikov, V.V., 1974. Velocity field of convective cell in a horizontal liquid layer at thermogravitational convection. Izvestiya Acad. Nauk SSSR, Physics of atmosphere and ocean 10, 137–145.

Prakash, A., Koster, J.N., 1996. Steady Rayleigh-Bernard convection in a two-layer system of immiscible liquids. Trans. ASME J Heat Transfer 118, 366–373.

Prakash, A., Koster, J.N., 1997. Steady natural convection in a two-layer system of immiscible liquids. Int. J. Heat Mass Transfer 40, 2799–2812.

Richer, F.M., 1979. Focal mechanisms and seismic energy release of deep and intermediate earthquakes in the Tonga Kermadec region and their bearing on the depth extent on mantle flow. J. Geophys. Res. 84, 6783–6795.

Richer, F.M., McKenzie, D.P., 1981. On some consequences and possible causes of layered mantle convection. J. Geophys. Res. 86, 5142–6135.

Tolstykh, A.I., 1991. Algorithms for calculating incompressible flows with compact third-order approximations. In: Modern problems in computational aerodynamics. CRC Press, Boca Raton, pp. 103–129.

de Vahl Davis, G., 1983. Natural convection of air in a square cavity. Int. J. Numer. Meth. Fluids 3, 249–264.

de Vahl Davis, G., Jones, I.P., 1983. Natural convection in a square cavity: a comparison exercise. Int. J. Numer. Meth. Fluids 3, 227–248.

Yanenko, N.N., 1971. The Method of Fractional Steps. The Solution of Problems of Mathematical Physics in Several Variables. Springer-Verlag, Berlin.